International Journal of Psychophysiology 130 (2018) 63–72

Contents lists available at ScienceDirect

International Journal of Psychophysiology

journal homepage: www.elsevier.com/locate/ijpsycho

Diminished neural network dynamics in amnestic mild cognitive impairment

Einat K. Brenner[a,b,*], Benjamin M. Hampstead[f,h,i], Emily C. Grossner[a,b], Rachel A. Bernier[a,b], Nicholas Gilbert[a,b], K. Sathian[a,c,d,e,f,g], Frank G. Hillary[a,b,c]

[a] Department of Psychology, The Pennsylvania State University, University Park, PA, United States
[b] Social, Life, and Engineering Sciences Imaging Center, University Park, PA, United States
[c] Department of Neurology, Penn State College of Medicine, Hershey, PA, United States
[d] Rehabilitation R&D Center, Atlanta VAMC, United States
[e] Department of Neurology, Emory University, United States
[f] Department of Rehabilitation Medicine, Emory University, United States
[g] Department of Psychology, Emory University, United States
[h] VA Ann Arbor Healthcare System, University of Michigan, United States
[i] Department of Psychiatry, University of Michigan, United States

ARTICLE INFO

Keywords:
fMRI
Memory
Dynamic connectivity
Graph theory
mild cognitive impairment

ABSTRACT

Mild cognitive impairment (MCI) is widely regarded as an intermediate stage between typical aging and dementia, with nearly 50% of patients with amnestic MCI (aMCI) converting to Alzheimer's dementia (AD) within 30 months of follow-up (Fischer et al., 2007). The growing literature using resting-state functional magnetic resonance imaging reveals both increased and decreased connectivity in individuals with MCI and connectivity loss between the anterior and posterior components of the default mode network (DMN) throughout the course of the disease progression (Hillary et al., 2015; Sheline & Raichle, 2013; Tijms et al., 2013). In this paper, we use dynamic connectivity modeling and graph theory to identify unique brain "states," or temporal patterns of connectivity across distributed networks, to distinguish individuals with aMCI from healthy older adults (HOAs). We enrolled 44 individuals diagnosed with aMCI and 33 HOAs of comparable age and education. Our results indicated that individuals with aMCI spent significantly more time in one state in particular, whereas neural network analysis in the HOA sample revealed approximately equivalent representation across four distinct states. Among individuals with aMCI, spending a higher proportion of time in the dominant state relative to a state where participants exhibited high cost (a measure combining connectivity and distance), predicted better language performance and less perseveration. This is the first report to examine neural network dynamics in individuals with aMCI.

1. Background

Mild cognitive impairment (MCI) is widely regarded as an intermediate stage between typical aging and dementia, with about 30% of MCI patients converting to Alzheimer's dementia (AD) and nearly 50% of individuals with amnestic MCI (aMCI) converting to AD within a 30-month follow-up period (Fischer et al., 2007). Patients with aMCI are characterized by impairments in learning and memory, though additional cognitive deficits are often evident depending on when an individual presents clinically (Albert et al., 2011).

Resting-state functional magnetic resonance imaging (rs-fMRI) examines coherent oscillations of low frequency fluctuations in the blood oxygen level-dependent (BOLD) signal, thereby allowing for the identification of sets of regions whose activity is correlated when an individual is not engaging in any particular task (Biswal et al., 1995; Gusnard and Raichle, 2001). Using this method, there is now a large literature demonstrating a gradual loss of connectivity between anterior and posterior brain regions in AD, but this disconnection may be preceded by a mix of increased and decreased connectivity in individuals with MCI (Badhwar et al., 2017; Hillary et al., 2015; Sheline and Raichle, 2013; Tijms et al., 2013). Specifically, early disease states may result in hyperconnectivity in areas of the default mode network (DMN) (Hillary et al., 2015), a group of brain regions including the posterior cingulate cortex and the ventromedial prefrontal cortex that is believed to be involved in self-referential thought and memory processing (Raichle et al., 2001; Raichle, 2015). Other disruptions in connectivity

* Corresponding author at: Department of Psychology, The Pennsylvania State University, University Park, PA, United States.
E-mail address: ebb5161@psu.edu (E.K. Brenner).

https://doi.org/10.1016/j.ijpsycho.2018.05.001
Received 8 December 2017; Received in revised form 22 March 2018; Accepted 2 May 2018
Available online 05 May 2018
0167-8760/

Table 1
Demographics.

	Age (years)	Education (years)	Gender	Race
aMCI (n = 43)	71.77 ± 7.23 (55–88)	16.12 ± 2.75	21 F, 22 M	24 W, 16 B, 3 L
HOA (n = 33)	69.52 ± 7.73 (59–86)	16.61 ± 1.94	29 F, 4 M	23 W, 10 B

Data are expressed as mean ± standard deviation (range). No significant between-group differences in age ($p = 0.186$) and education ($p = 0.468$) were found (two-tailed). One individual's gender was not reported. W = white, B = black, L = latinx. This table represents demographics for the aMCI group excluding the individual who was excluded due to excessive movement.

within the hippocampus (Jones et al., 2016), posterior cingulate cortex (Brier et al., 2012), and medial temporal lobes (Dickerson and Sperling, 2008) have been associated with reduced memory performance. Furthermore, hubs in the cognitive control (CC) network, which includes the anterior cingulate cortex, dorsolateral prefrontal cortex, and posterior parietal cortex (Cole and Schneider, 2007), have shown increases in connectivity in individuals with AD when compared to healthy controls (Agosta et al., 2012; Hillary et al., 2015). Disease onset therefore presents as hyperconnectivity that degrades as the disease develops, cascading from posterior to anterior connectivity degradation (Damoiseaux et al., 2012; Hillary and Grafman, 2017; Jones et al., 2016).

In order to characterize distributed neural networks, investigators have combined rs-fMRI methods with graph theory, an applied mathematical approach permitting analysis of all possible connections across the network (Bassett and Bullmore, 2006). Recent application of graph theory methods in the study of aMCI has revealed an overall decrease in connectivity, which is commonly observed as an overall increase of average path length, or a decrease in the global efficiency of the network (Wang et al., 2013). Wang and colleagues also observed that participants with aMCI exhibited decreased modularity, a community structure metric characterized by groups of nodes densely linked among themselves and more sparsely linked to nodes outside the local grouping. Two related dimensions of network functioning may be affected in aMCI. First, there is a nonlinear trend in connectivity change, with enhanced connectivity early on in the disease giving way to connectivity loss based upon the degree of cortical atrophy (de Haan et al., 2009). Second, information processing via network hubs declines as connectivity is lost and modularity, or "community structure," degrades (for review see Hillary and Grafman, 2017).

To date, network studies in MCI, including those using graph theory, have investigated neural networks by quantifying the relationship (e.g., a single correlation coefficient) between any two nodes for the entire data collection period. This method assumes temporal and spatial stationarity in the relationship between network nodes over the course of the time series. New approaches such as dynamic connectivity, which have been applied to other clinical populations such as mild traumatic brain injury (TBI) (Mayer et al., 2015) and schizophrenia (Braun et al., 2016; Rashid et al., 2014), allow for increased sensitivity to subtle temporal variations that can be missed when correlating two time series. A relatively new method examining dynamic functional connectivity works by identifying brain states that neural networks transition through during resting state in the absence of any externally imposed task. In this paper, we examine dynamic functional connectivity by studying smaller windows of time to gain access to these brain states. We seek to understand the different resting-state profiles of individuals with aMCI compared to healthy older adults (HOAs), with a focus on network dynamics and flexibility as neural systems move between distinct connectivity states. To our knowledge, no other study has examined dynamic connectivity in individuals with aMCI.

1.1. Study goals and hypotheses

The goal of this paper is to compare dynamic functional connectivity brain states during rest between individuals with aMCI and HOAs. We focus on proportion of time spent in distinct brain states as well as transitions between distinct states based upon a dynamic functional connectivity analysis.

Overall, we hypothesized that compared to HOAs, individuals with aMCI will show network dynamics marked by fewer transitions between states and state attendance that is concentrated more heavily on one state instead of spread out across many. This hypothesis is based on previous literature demonstrating that diminished network variability has been observed after traumatic brain injury (TBI) (Nenadovic et al., 2008) where there exists challenges to neural network resources. Second, we predicted that hub regions within the DMN and CC network would function as "drivers" for the proportion of time spent in the most common state in the aMCI sample. Finally, given the above noted evidence of a posterior to anterior loss of long-distance connectivity in MCI, we predicted that diminished connectivity in posterior hubs in the aMCI sample would predict cognitive deficit (Brier et al., 2012; Dennis and Thompson, 2014; Li et al., 2013; Sorg et al., 2007).

2. Materials and methods

2.1. Procedure

Subjects included 44 individuals diagnosed with aMCI and 33 HOAs of comparable age and education (Table 1). Subjects with aMCI were recruited from the Atlanta Veterans Affairs Medical Center (VAMC) as well as the Emory University Alzheimer's Disease Research Center (ADRC). Those with aMCI were diagnosed according to the Petersen criteria (Petersen, 2004) via consensus conferences that included neurologists, geriatricians, neuropsychologists, and other clinical staff, who took into account laboratory results, neuroimaging, neuropsychological, and other test results as available. HOA participants were recruited from the Emory ADRC as well as the general Atlanta metropolitan area. These participants were determined to have normal cognition using the same consensus approach. General exclusion criteria included any other neurologic injury or disease, psychiatric disorders, and current or past alcohol or drug abuse or dependence. All of the data were collected at Emory University, and all participants gave written, informed consent. The study was approved by the Institutional Review Board of Emory University and the Research and Development Committee of the Atlanta VAMC.

2.2. Behavioral data

Given the time lag that can occur between diagnosis and study enrollment, all participants completed a standard neuropsychological protocol, described below, at the time of study enrollment. This ensured that patients with aMCI did not convert to AD or revert to normal and that HOAs were still cognitively intact. This protocol included the Mini-Mental State Examination (MMSE), the Repeatable Battery for the Assessment of Neuropsychological Status (RBANS), the Wechsler Test of Adult Reading (WTAR), the Trail Making Tests A and B (Trails-A and Trails-B), and the Emory Version of the Wisconsin Card Sorting Test (EWCST). Table 2 reports means and standard deviations of neuropsychological test results for both groups, providing a good clinical indicator of disease severity in this cohort. In order to minimize

Table 2
Raw scores of neuropsychological performance of aMCI and HOA groups.

	aMCI (n = 43)	HOA (n = 33)
MMSE*	**28.20 ± 1.98**	**29.39 ± 0.97**
WTAR-FSIQ	109.52 ± 13.32 (77–125)	109.52 ± 9.21 (86–122)
RBANS ImMem*	**86.71 ± 15.59**	**108.00 ± 10.08**
RBANS VisCon	**97.19 ± 16.58**	**102.09 ± 14.02**
RBANS Lang*	**91.26 ± 17.03**	**104.06 ± 11.33**
RBANS Attn*	**97.71 ± 14.30**	**106.06 ± 14.79**
RBANS DelMem*	**82.43 ± 18.24**	**104.76 ± 11.59**
RBANS Total*	**88.50 ± 12.04**	**106.79 ± 11.66**
Trails-A	48.22 ± 10.49	49.64 ± 9.70
Trails-B	49.40 ± 11.32	51.36 ± 10.02
EWCST InStrat	2.63 ± 0.63	2.81 ± 0.40
EWCST TotSort*	**3.68 ± 1.80**	**4.66 ± 1.33**
EWCST TotErr*	**17.93 ± 10.22**	**13.00 ± 4.72**
EWCST PersErr*	**5.75 ± 6.94**	**2.22 ± 2.88**
EWCST SLErr	1.31 ± 1.66	1.31 ± 1.47

Data are expressed as mean ± standard deviation (range). A '*' indicates significant between-group differences, $p < 0.05$ (two-tailed). "ImMem" = Immediate Memory, "VisCon" = Visual Construction, "Lang" = Language, "Attn" = Attention, "DelMem" = Delayed Memory, "Total" = Total Score, "InStrat" = Initial Strategies, "TotSort" = Total Number of Categories Sorted, "TotErr" = Total Errors, "PersErr" = Total Perseverative Errors, "SLErr" = Total Set Loss Errors. This table represents demographics for the aMCI group excluding the individual who was excluded due to excessive movement.

comparisons, we chose five tests for further analyses: the RBANS Language Index Score, RBANS Delayed Memory Index Score, and the Perseverative Errors, Set Loss Errors, and Total Categories Sorted from the EWCST. The RBANS Language Index Score was chosen because a language deficit is an early sign of AD (Caccappolo-Van Vliet et al., 2003; Lukatela et al., 1998; Martin and Fedio, 1983; Williams et al., 1989). Furthermore, the RBANS Delayed Memory Index Score was chosen for analyses due to the amnestic nature of the MCI subtype of participants. We also examined two of the error measures from the EWCST due to their sensitivity to executive deficits in the MCI and AD populations (Bondi et al., 1993; Nagahama et al., 2003). Lastly, we examined the total number of categories completed, as Bondi and colleagues found it to be the strongest discriminative subtest for patients with AD (1993).

2.3. MRI parameters

All scans were conducted on one of two Siemens Trio 3T MRI scanner machines using a 12-channel head coil. Both machines were used for the Alzheimer's Disease Neuroimaging Initiative (ADNI) and were designed to be interchangeable. Data from all HOA participants and three participants with aMCI were collected on one scanner, while data for the remainder of the individuals with aMCI were collected on the second scanner. High-resolution anatomical images were taken using a three-dimensional magnetization-prepared rapid acquisition with gradient echo (MPRAGE) sequence (repetition time (TR) = 2300 ms, echo time (TE) = 3.0 ms, inversion time = 1100 ms, flip angle (FA) = 8°). This led to 176 sagittal slices of 1 mm thickness (field of view (FOV) = 256 mm, in-plane resolution = 1 × 1 mm, in-plane matrix = 256 × 256). BOLD contrast T2*-weighted functional images were obtained using single-shot, gradient-recalled, echo-planar imaging (EPI) sequences with the following parameters: TR 2000 ms, TE 30 ms, FOV 220 mm, FA 90°. 29 axial slices of 4 mm thickness were each obtained with an in-plane resolution of 3.4 × 3.4 mm^2 and an in-plane matrix of 64 × 64.

2.4. fMRI data preprocessing

A time series of 210 volumes of data was collected during an 8-minute rest period. In order to control for signal instability, the first five volumes were removed for each subject, leaving 205 volumes. All preprocessing steps were conducted in SPM8 (www.fil.ion.ucl.ac.uk/spm/software/spm8/). Next, all volumes were slice-time corrected and realigned in SPM8. Using the ArtRepair toolbox, spike artifacts were removed based on a 17-point moving average of unfiltered data. High-pass filtering was avoided to allow for examination of the ratio of high- to low-frequency oscillations in the BOLD signal during independent component analysis (ICA). Each subject's high-resolution (1 × 1 × 1 mm) T1 image was coregistered to the mean functional image in SPM8. This coregistered image was then segmented in SPM8, resulting in a normalized, gray matter image in MNI space. The functional images were normalized to the MNI space and these normalized images along with the gray matter image were resliced into voxel dimensions of 3 × 3 × 3 mm. Smoothing was completed using a Gaussian filter (full width kernel at half maximum 6 mm), in order to improve the signal-to-noise ratio and reduce ringing artifacts (Lindquist, 2008). Head motion correction was conducted using the ArtRepair toolbox. ArtRepair detected one individual with aMCI who displayed head motion in > 20% of their total volumes (~30%). Although analyses with and without this individual were not significantly different, their data was removed after the ICA step. Percent of volumes repaired for participants with aMCI (M = 4.34; SD = 7.74) and HOAs (M = 0.40; SD = 0.01) were in the acceptable range.

2.5. Analytic approach and pipeline

2.5.1. Whole-brain mask

A whole brain mask was created using images from all participants, regardless of group. We resliced the segmented white matter, gray matter, and CSF masks using SPM8. These were then mapped onto the average smoothed, normalized functional image for each subject. The resliced masks were summed and then binarized using the fMRIB Software Library (FSL; http://fsl.fmrib.ox.ac.uk). As described later, we analyzed coordinates that peaked in gray matter, consistent with our questions about connectivity.

2.5.2. Independent component analysis (ICA)

After data were preprocessed, the GIFT toolbox (www.mialab.mrn.org/software/gift) was used to organize both groups together into spatially independent components using group-level specific ICA. We used a high model order of 100 components using the whole-brain mask in order to ensure whole-brain parcellation (Allen et al., 2014). 100 components have been used in the literature, with certain groups discussing the advantage of a relatively high order model (Abou-Elseoud et al., 2010; Kiviniemi et al., 2009; Smith et al., 2009). The investigators sought to track the most robust and reliable regions within large subnetworks and anticipated that ICA would provide reliable network estimation, as discussed by Calhoun and colleagues (2009).

Two investigators, E.K.B. and F.G.H., independently examined the components outputted from the GIFT toolbox. Components were chosen taking into account the following criteria: a high ratio of low-frequency to high-frequency fluctuations, lack of spatial fragmentation, minimal spatial overlap with CSF, and peak connectivity in gray matter (Cordes et al., 2000; Allen et al., 2014). Each investigator first chose the components separately, and then components in which there was a disagreement were discussed until consensus was reached. This selection process resulted in 46 useable components for dynamic connectivity analyses (Fig. 1). Lastly, to identify component labels, peak coordinates were mapped onto the Harvard-Oxford atlas within FSL (Desikan et al., 2006; Smith et al., 2004; https://fsl.fmrib.ox.ac.uk/fsl/fslwiki/). The peak coordinates were identified based on the peak of distribution. Based on these labels as well as functional network labels assigned by the GIFT toolbox, components were sorted into one of six networks: the auditory network (AUD), the cognitive control network (CC), the basal ganglia network (BG), the visual network (VIS), the motor network

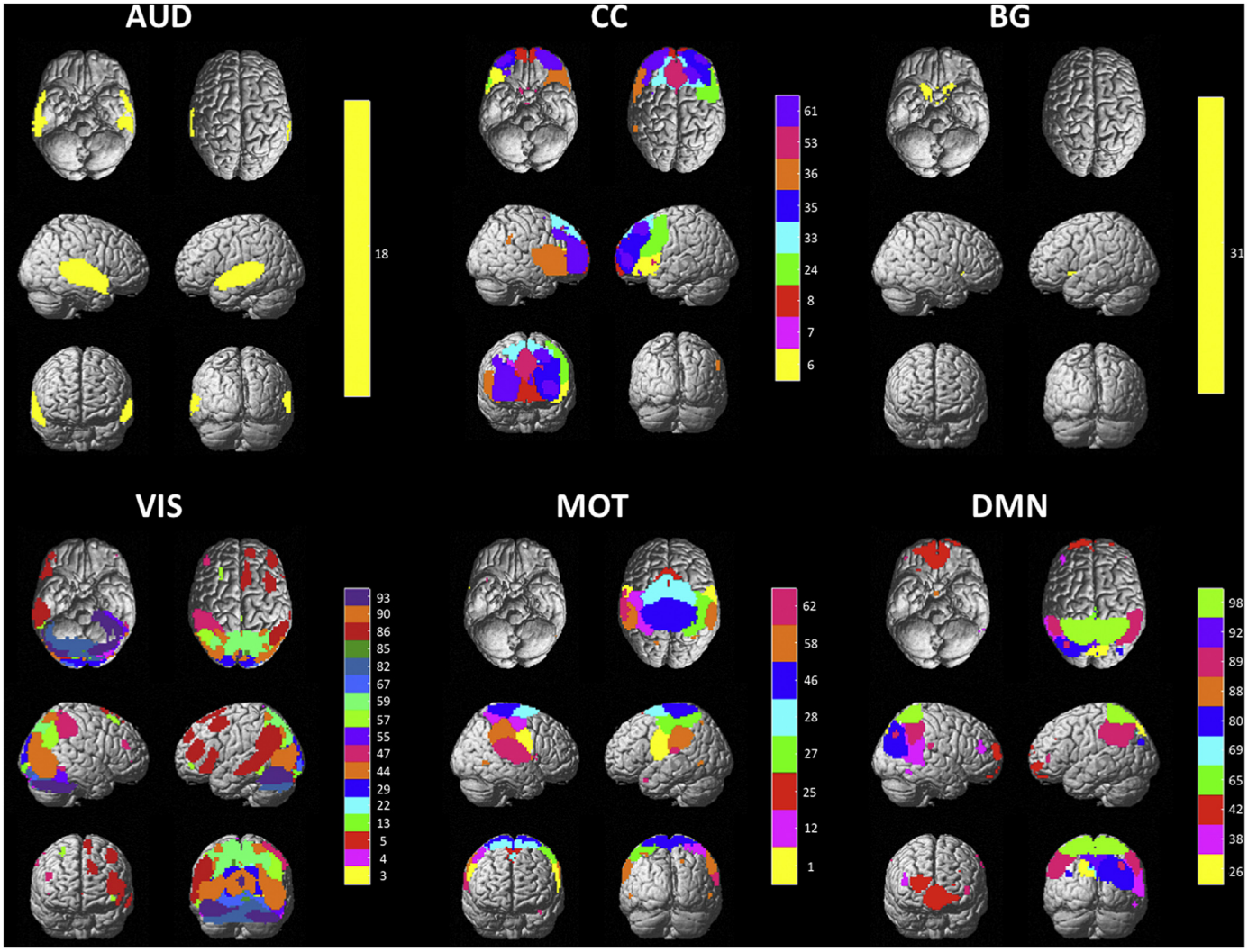

Fig. I. This figure illustrates the output of the ICA, which resulted in 46 usable components. These components were sorted into the six networks shown in this figure. The bar to the right of each network illustrates different component numbers, which can also be examined in Fig. II. "AUD" = Auditory Network, "CC" = Cognitive Control Network, "BG" = Basal Ganglia Network, "VIS" = Visual Network, "MOT" = Motor Network, "DMN" = Default Mode Network.

(MOT), and the default mode network (DMN).

2.5.3. Dynamic network analysis

Using the subject-wise static maps created in the initial ICA step, we used the dynamic functional network connectivity (dFNC) toolbox in GIFT to examine the dynamic nature of resting state connectivity for all subjects. All 46 components were de-trended for each subject, and a low-pass filter at a high-frequency cutoff of 0.15 Hz was used. dFNC was calculated using the "sliding window" approach, with a window step size of 15 volumes (30 s), which allows for sampling overlapping windows of time during the time series. Previous work has shown little effect on dynamic connectivity when varying window sizes between 30 s and 2 min (Chang and Glover, 2010; Hutchison et al., 2013). Each session contained 205 volumes per subject, resulting in time courses of 410 s (TR = 2 s) each. Using an L1 regularization, a window step size of 15 volumes (30 s) was implemented. The L1 regularization step is adapted from Allen and colleagues (2014). Because of the diminished variance represented in smaller windows, a precision matrix (inverse covariance) is used. The L1 regularization operates as a loss function that is minimized to avoid overfitting the data and to encourage network sparsity while providing the most robust estimate of the covariance matrix (Allen et al., 2014). The dFNC windows resulting from the above process were then clustered using a k-means algorithm (Lloyd, 1982), and Euclidean distance was used to cluster the data into five states. A k-means value of five was chosen because it was the largest value where no state was attended by only a single subject, and we had interest in maximizing states, even with risk of cluster heterogeneity. Of these five states, four were chosen for analysis due to their proportion of time spent in each state (> 10%) across all subjects (i.e., participants spent time in these brain states for > 10% of the duration of the time series). This resulted in metrics such as proportion of time spent in each state as well as number of state transitions (Allen et al., 2014). Time spent in each state was calculated across all subjects, despite the fact that not all participants entered each state. Therefore, if an individual did not enter a state, their proportion of time spent there was included in analyses as 0.

2.5.4. Graph theory metrics and analysis

In our dynamic analyses, we examined the costs of various hubs during particular states using graph theory. The following is a conceptual explanation of those calculations.

In graph theory, a *node* is defined as a brain region or region of interest (ROI). The connection, or *edge*, is the functional relationship between two nodes. The *degree* of a node is the number of connections coming out of it. We wanted to take into account not only the number of connections nodes had to each other, but also their strengths. Thus, we

looked at *weighted degree*, the strength of the relationship, or Pearson correlation, for a corresponding pair of nodes. In a weighted graph, the degree of a node is the sum of the weights of all the node's edges. By summing the weights of edges within a network, we calculate the *network strength*. Thus, a *hub* can be thought of as a node with high degree or high centrality.

Our definition of *network cost* is based on the assumption that connections between ROIs that are physically farther away from each other in the graph are more metabolically expensive than connections between ROIs a shorter distance apart (Liang et al., 2013). In this calculation, we defined the cost of each edge as the product of the Euclidean distance between the pair of ROIs that it connects and the absolute weight of that connection (Roy et al., 2017). Using this definition, nodal cost is the sum of all edge costs, where the cost of each edge is the product of Euclidean distance by the correlation value. For network cost, the cost of every edge is aggregated for the entire network. In doing so, this definition of cost takes into account connection strength, Euclidean distance within the graph, and number of connections. The goal was to determine network nodes showing the highest and lowest cost when comparing the MCI group to the HOA sample.

2.5.5. Network and behavioral analysis

To determine the relationship between measures of network dynamics and cognitive functioning, we conducted first-order Pearson correlations. In order to reduce the number of comparisons, we examined the relationship between dynamic neural network measures and cognitive functioning on five pre-selected tests: the RBANS Language Index Score, RBANS Delayed Memory Index Score, and the Perseverative Errors, Set Loss Errors, and Total Categories Sorted from the EWCST. The reasons for choosing these tests were discussed above in the Behavioral data section. Correlational analyses were conducted between these five cognitive tests and two levels of network analysis: 1) state-level data based upon between-group differences, and 2) regional connectivity of areas determined to be hyper- and hypo-connected. Bonferroni statistical corrections for multiple comparisons were made within each of these sub-analyses.

3. Results

3.1. Analysis plan

An important emphasis in the analytic plan was to focus on within-group metrics describing functional network change and the role of critical hubs in driving the most occupied brain states in individuals with aMCI. Thus, we rely sparingly on between-group comparisons and only to provide context.

3.2. Spatial extent of components and adjacency matrices for states

Fig. II displays the adjacency matrix for each state, including a visualization of all components, and Fig. III depicts the correlation matrix of positive and negative connections for each state.

3.3. Proportion of time spent and transitions

Analysis examining five network states revealed that states 2, 3, 4, and 5 were the states where subjects in both groups spent a considerable proportion of their time (each > 10% of duration of rest, for both populations, see Table 3). State 1 was omitted from further analysis due to its low proportion of time spent by the aMCI group (< 10%). Within-group one-sample *t*-tests revealed that participants with aMCI spent a high amount of their time in state 4 (M = 46.2%, SD = 0.35). In fact, the aMCI group spent significantly more time in state 4 than in state 2 ($t(42) = 4.23$, $p < 0.001$, $d = 1.09$), state 3 ($t(42) = 5.06$, $p < 0.001$, $d = 1.24$), or state 5 ($t(42) = 3.46$, $p < 0.01$, $d = 0.90$) (Table 3). These findings remained significant after correcting for multiple comparisons using a Bonferroni correction, $p < 0.013$. In the HOA group, state 2 was the most commonly attended state (M = 26.8%; SD = 0.030) (Table 3). One-sample *t*-tests showed that time spent in state 2 for HOAs was not significantly different from time spent in state 3 ($t(32) = 0.99$, $p = 0.332$, $d = 0.27$), state 4 ($t(32) = 0.41$, $p = 0.684$, $d = 0.11$), or state 5 ($t(32) = 0.80$, $p = 0.428$, $d = 0.23$) (Table 3). As such, the aMCI group spent much more of their time concentrated in one state, while the HOA group spent similar durations of time among all states. Interestingly this finding did not translate to differences in transitions; the aMCI and HOA groups did not differ significantly in the number of between-state transitions, ($t(72) = 0.13$, $p = 0.897$, $d = 0.03$).

In order to test the robustness of the findings with respect to transitions and proportion of time spent (including single-state dominance in the aMCI sample), we examined these parameters across a range of k-cluster values. The pattern where individuals with aMCI spent much more of their time concentrated in one state while the HOA group spent their time more equally across states was observed regardless of the assigned k-means cluster value (Fig. IV and Appendix A). The finding that there was no significant difference in number of transitions between groups was also consistent regardless of k-cluster value (Appendix B). Therefore, we anticipate that the selection of k = 5 did not influence the findings. Given that state 4 was the most common state in the aMCI group, we focused additional analyses on this state.

When examining cost, the cost of posterior DMN and CC regions during state 4 was significantly lower for the MCI group than in state 2 ($t(8) = 11.38$, $p < 0.001$, $d = 1.97$), state 3 ($t(8) = 6.27$, $p = 0.0002$, $d = 1.94$), and state 5 ($t(8) = 7.38$, $p < 0.001$, $d = 2.16$) (Fig. V). This held true following correction for multiple comparisons using a Bonferroni correction, $p < 0.013$. This may indicate that the MCI group gravitates toward a low-cost state, at least in certain key posterior DMN regions (e.g., PCC).

3.4. State proportion of time spent and performance

In individuals with aMCI, the proportion of time spent in state 4, the most dominant network state, did not predict cognitive function. Therefore, we explored how the proportion of time spent in the most dominant state relative to higher cost states predicted cognition. To do so, we examined the relationship between the ratio of time spent in state 4 (the most common state) and state 2 to cognitive function using a Pearson's correlation. We chose state 2 because, as Fig. V illustrates, state 2 was the most costly state when examining posterior DMN and CC network components; the same held true when examining the average costs of anterior and posterior DMN and CC network components. The ratio of time spent in state 2 to time spent in state 4 (SD = 2.08; range = 0.02–7.79) was not significantly associated with cognitive performance.

Since state 3 showed the second-highest posterior cost in the aMCI group, and its cost was also significantly higher than that of state 4, ($t(8) = 6.27$, $p = 0.0002$, $d = 1.94$), we then used a Pearson's correlation to examine whether the ratio of time spent in state 3 to state 4 (SD = 2.73; range = 0.18–8.82), was significantly associated with performance. Results showed that the proportion of time spent in state 3 to state 4 was significantly positively associated with performance on the RBANS Language index, ($p = 0.034$, $R^2 = 0.41$). This proportion was also significantly negatively associated with the number of perseverative errors on the EWCST ($p = 0.015$, $R^2 = 0.54$) (Table 4). Thus, a higher proportion of time spent by aMCI participants in state 3 relative to the most dominant state (state 4) was associated with enhanced performance.

We further examined the relationship between proportion of time spent in state 5 to state 4 and performance on the RBANS Language index and EWCST Perseverative Errors in order to determine if this effect was specific to the time spent in state 3 relative to state 4. These two relationships were exclusive to the proportion of time spent in state

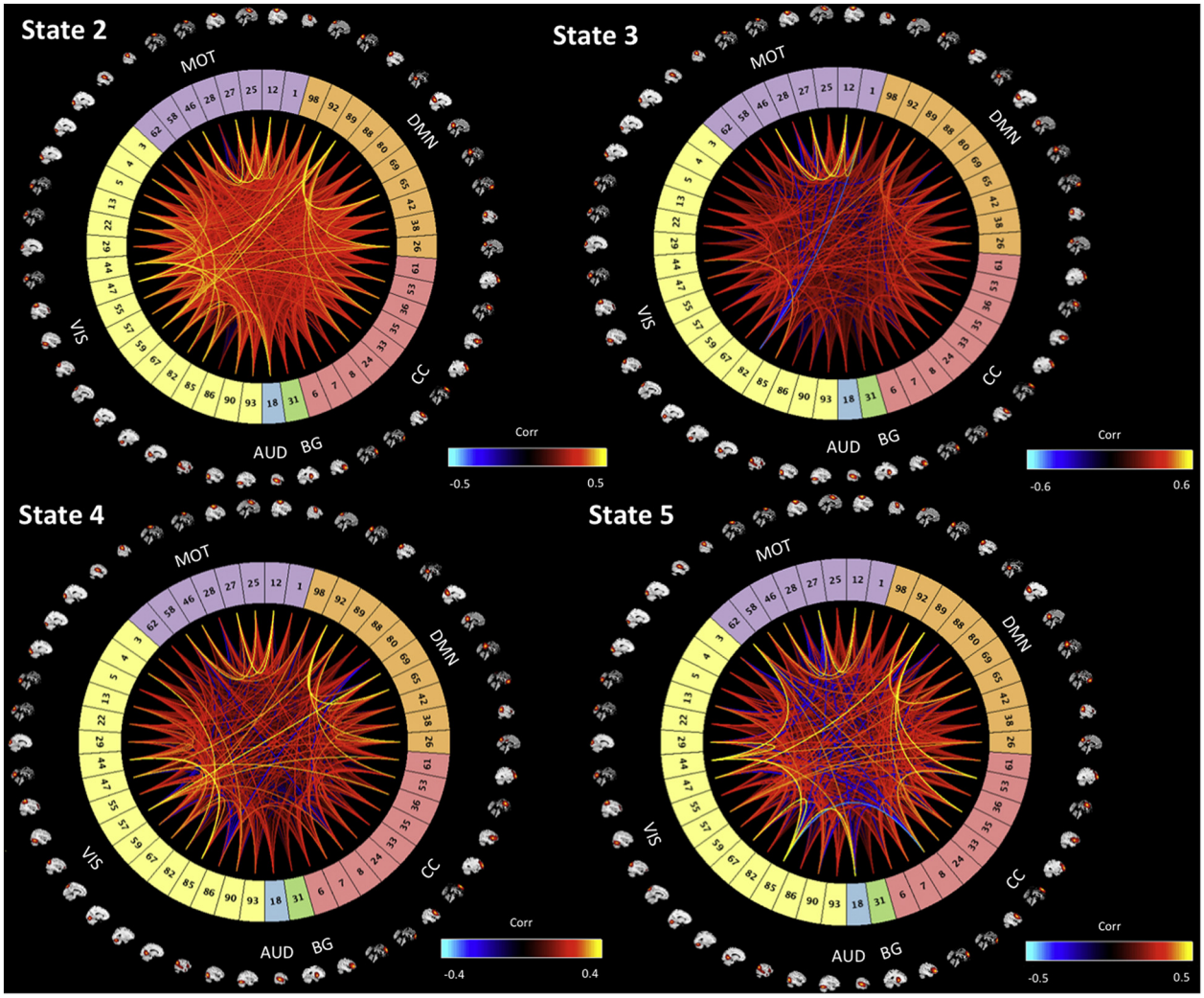

Fig. II. This figure demonstrates the connectivity profile of each analyzed state, including a visualization of all components used. Component numbers are identical to those used in Fig. I. "AUD" = Auditory Network, "CC" = Cognitive Control Network, "BG" = Basal Ganglia Network, "VIS" = Visual Network, "MOT" = Motor Network, "DMN" = Default Mode Network.

3 relative to state 4.

In an additional exploratory analysis, we examined whether the two relationships between performance and proportion of time spent in state 3 relative to state 4 were present in the HOA group using Pearson's correlations. These analyses yielded null results for the RBANS Language composite, ($p = 0.250$, $R^2 = 0.18$), but a significant relationship with EWCST Perseverative Errors was present, ($p = 0.002$, $R^2 = 0.76$).

3.5. Overall network hubs and dominant state

In order to examine the role of network hubs in facilitating the proportion of time spent in various states, we examined the most costly nodes in state 4, the state with the highest proportion of time spent in the aMCI group. To test the hypotheses regarding posterior disconnection in critical subnetworks including the DMN and CC network, we focused on the most costly and least costly nodes. These were defined as the nodes with a cost 1.5 standard deviations above and below the mean aMCI component cost, respectively. Analyses revealed that cost in these sets of nodes did not correlate significantly with the proportion of time spent in state 4. Therefore, the most commonly attended state in the aMCI group did not appear to be driven by the most highly connected anterior or posterior regions.

3.6. Posterior hubs and behavior

For this within-group analysis, we focused on posterior hubs and anti-hubs in state 4 when examining correlations between hubs and behavior. This was driven both by the dominant nature of state 4 in this group as well as the aforementioned posterior dropout in the MCI literature. A hub or anti-hub was defined as a component with a cost one standard deviation above or below the average posterior component cost for the aMCI group, respectively; in other words, an anti-hub indicated a region that was disconnected relative to all other posterior components. This revealed two posterior hubs and one posterior anti-hub. Cost in these areas did not predict behavior.

4. Discussion

The primary goal of this study was to examine the dynamic brain states arising in individuals with aMCI and to determine if these states served as predictors of cognitive outcome. The primary findings reveal that participants with aMCI reliably demonstrated brain dynamics characterized by a single state dominating nearly half of the rest-period activity (state 4) and a second, less frequently attended state characterized by relatively higher network cost (state 3). We focused additional analyses on these two network states, including their ratios to one another and how these brain dynamics predicted behavior. Finally,

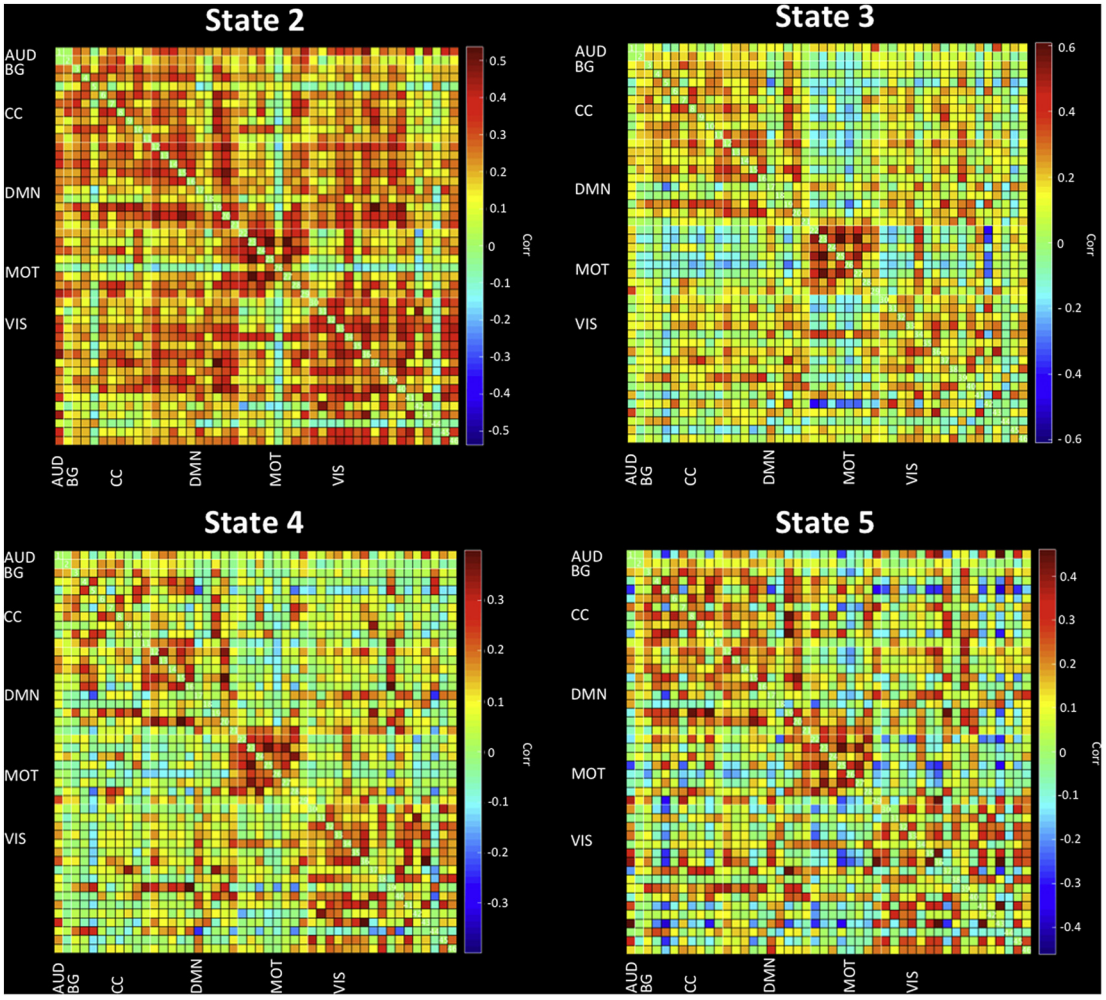

Fig. III. This figure depicts the correlation matrix of positive and negative connections for each analyzed state. "AUD" = Auditory Network, "CC" = Cognitive Control Network, "BG" = Basal Ganglia Network, "VIS" = Visual Network, "MOT" = Motor Network, "DMN" = Default Mode Network.

it was a goal to examine the role that network hubs played in driving brain states. Interestingly, however, the findings did not support the hypothesis that network hubs would function as "drivers" of proportion of time spent in states and predictors of cognitive outcome. These findings are integrated with a broader literature below.

4.1. State proportion of time spent

Our results yielded four dominant network states that were included in initial analyses. State 4 was the most commonly attended state in the aMCI group, as individuals spent significantly more time there than any other state. This pattern was not evident in the HOA sample, which saw relatively even distribution across four common brain states.

Although there is minimal literature on network variability within the MCI population, diminished network variability has been observed after TBI (Nenadovic et al., 2008; Gilbert et al., 2018). Additionally, variability in brain signaling has been linked to greater cognitive recovery in individuals who sustained a TBI (Beharelle et al., 2012). An analysis of cost in the posterior areas of the DMN and CC network demonstrated that state 4, which the MCI group heavily attended, exhibited significantly lower cost than other states. Diminished connectivity in neural networks has been widely observed in MCI (Bai et al., 2012; Binnewijzend et al., 2012; Rombouts et al., 2005). Overall, the network stability seen in the aMCI group is consistent with changes seen in other forms of neurological injury and portends a poor cognitive outcome.

We anticipated that the relative inflexibility for the aMCI sample to move from state 4 (most common state) to the intermittent occurrence of a significantly more costly state had consequences for cognition, so we first examined the ratio of time spent in state 2 relative to state 4, as state 2 was the state with the highest cost. The relative proportion of time spent in state 2 to that spent in state 4 did not have an association

Table 3
Proportion of time spent and number of transitions.

	State 2	State 3	State 4	State 5	Transitions
aMCI	0.147 ± 0.218	0.112 ± 0.201	0.462 ± 0.347*	0.182 ± 0.273	3.93 ± 2.88
HOA	0.263 ± 0.303	0.186 ± 0.269	0.228 ± 0.324	0.194 ± 0.314	3.85 ± 2.56

Data are expressed as mean ± standard deviation. The first four columns (State X) indicate the proportion of time spent in the respective state. The last column indicates the number of average transitions participants made between states. A '*' indicates a state that was occupied significantly more by a group when compared to the group's occupation of other states, $p < 0.05$ (two-tailed).

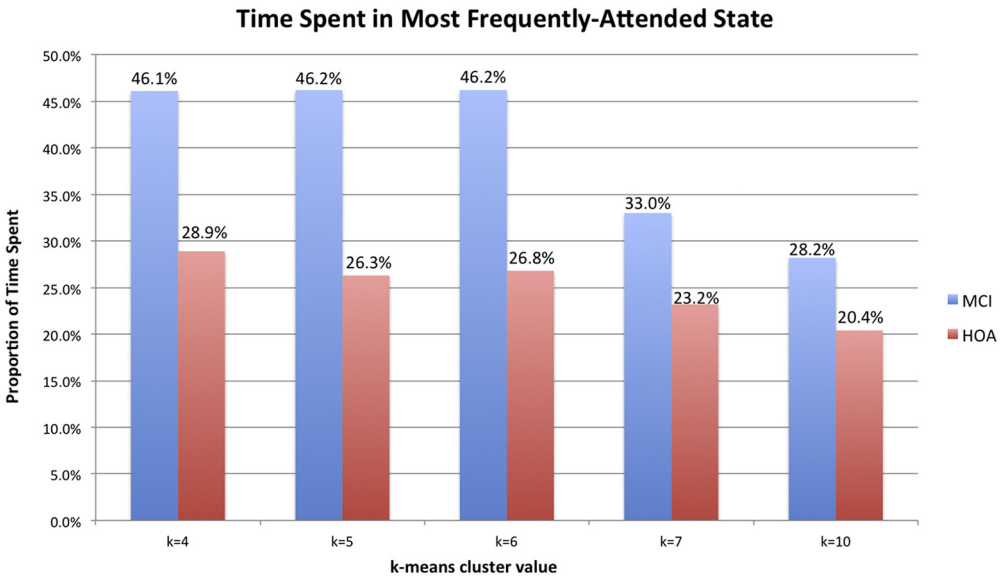

Fig. IV. This figure illustrates the proportion of time spent in the most dominant state for each k-means cluster value, for each of the two groups.

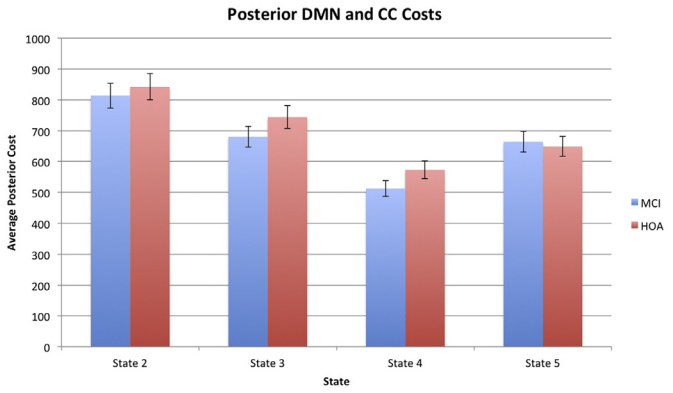

Fig. V. Examining only components in the DMN and CC network, this figure shows the average cost of posterior components.

Table 4
Proportion of time spent (ratios) and cognitive performance in aMCI.

Ratio	Measure	*p*-Value	R^2
P3/P4	RBANS DelMem	0.201	0.17
P3/P4	RBANS Lang	**0.034***	0.41
P3/P4	WCST PersErr	**0.015***	0.54
P3/P4	WCST SLErr	0.356	0.11
P3/P4	WCST TotSort	0.361	0.12

For measures of error, higher scores are indicative of worse performance. A "*" indicates statistical significance of $p < 0.05$ (two-tailed). "P3" = proportion of time spent in state 3. "P4" = proportion of time spent in state 4.

with cognitive performance. We therefore conducted these analyses in the state with the second-highest cost, state 3. Results showed that the ratio of the proportion of time spent in state 3 relative to state 4 significantly predicted a measure of language that included verbal fluency and picture naming. This ratio also had a strong relationship, accompanied by a strong effect size, with cognitive perseveration, which has been linked to mild AD (Bondi et al., 1993). This indicates that spending more time in state 3 relative to state 4 may signal the maintenance of language and less perseveration. These findings overall demonstrate that a higher proportion of time spent in state 3 may be an indicator of fewer cognitive deficits. State 3 was a state whose posterior cost was significantly greater than that of state 4, where individuals with aMCI spent the vast majority of their time. Although it is presently unclear what sets state 3 apart from states 2 and 5, spending time in state 3 relative to state 4 may indicate the possible engagement of residual resources during early disease progression. This was also true in the HOA population, where spending more time in state 3 relative to state 4 indicated less perseveration. In the current sample, individuals with aMCI spending more time in state 3 relative to state 4 showed fewer cognitive deficits, possibly by exploiting (at least transiently) a state with high posterior connectivity. Even so, these findings demonstrate that the relationship between brain state dynamics and measures of cognitive performance may not be entirely straightforward.

With respect to the meaning of the enhanced response observed in state 3, increased regional brain response commonly observed during goal directed behavior in neurological disorders, and even during normal aging, has historically been interpreted as neural compensation (Hillary et al., 2006; Dennis and Cabeza, 2008) or scaffolding (Park and Reuter-Lorenz, 2009). More recently, this finding has been extended to studies of network dynamics (Bernier et al., 2017; Medaglia, 2017). Based upon this explanation, the posterior connectivity loss observed in the MCI literature would be bolstered by greater anterior connectivity representing enhanced support via cognitive control (Hillary et al., 2006). One important observation counter to a compensatory explanation is that increased connectivity in the anterior hub, (e.g., frontal pole), was significantly correlated ($p < 0.05$) with connectivity in posterior hubs (e.g., angular gyrus, supramarginal gyrus), indicating a positive coupling as opposed to an accommodation in frontal systems for posterior connectivity loss. This finding is important and requires additional investigation including into the relationship between posterior and anterior hubs as neurodegeneration advances (Jones et al., 2016).

4.2. Whole brain hubs as drivers of brain states

There is a growing literature focused on the modular structure of brain networks with significant emphasis on the role of network hubs in facilitating subnetwork functioning and information transfer (van den Heuvel and Sporns, 2013). In order to investigate the role of network hubs as drivers of brain states, we determined the most costly nodes in state 4 for the aMCI group and examined these highly connected nodes in the context of proportion of time spent and cognitive outcome. The current data do not support regional hub response as a determinant of the proportion of time spent in state 4. This finding was surprising and

may be due to the nature of estimating dynamic states, where the role of any individual node is likely de-emphasized in favor of capturing the spatio-temporal fluctuations in the collective network response. Second, this finding could reflect the general diffusion of connectivity response across nodes in aging, which reduces the impact of individual nodes on a network; certainly there is some support of this in the healthy aging literature (Cabeza and Dennis, 2012). In order to investigate the connection between posterior dropout and performance more closely, we calculated posterior hubs and anti-hubs in state 4 for the aMCI group. However, cost in these hubs and anti-hubs also did not predict cognitive performance.

4.3. Limitations

There are a few limitations to this study. First, data from all HOAs were collected on one scanner and data from all but three of the participants with aMCI were collected on a separate scanner, which may introduce scanner-dependent group differences. However, the scanners were designed to be interchangeable with all of the same hardware and software and also underwent validation procedures as part of ADNI. We cannot rule out the possibility that the few between-group analyses were affected by the different scanners; however, our primary analyses were within-group and are therefore uncompromised. Also, there were no significant differences in average state costs in participants with aMCI whose data were collected on separate scanners. Future studies with a larger sample could replicate and extend our findings by distinguishing distinct stages of MCI (e.g., early vs. late), perhaps in conjunction with amyloid imaging. Finally, recent work has suggested that autoregressive models, not state-based models, may better explain dynamic connectivity (Liegeois et al., 2017). Future work should consider autoregressive models as an alternative strategy for estimating dynamic connectivity in clinical samples.

4.4. Conclusions and future research

The current study used dynamic functional connectivity to examine the distinct brain states that differentiate individuals with aMCI from their HOA counterparts. Connectivity analyses revealed that individuals with aMCI were more likely to spend time in a single dominant state, a finding that is consistent with the diminished network dynamics observed in other neurological disorders (Beharelle et al., 2012) and may be attributable to reduced flexibility in resource allocation. This result was independent of the assigned value of k used for the k-means clustering algorithm (Appendix A). Future research will focus on loss of neural network dynamics as a marker for conversion to AD. Furthermore, the finding that spending more time in a costly state relative to the most common state tends to mitigate language and perseveration deficits may provide insights into those transient states that permit preserved cognitive functioning as the disease progresses. This is especially promising given the fact that state 3 exhibited significantly higher posterior cost than state 4 in the aMCI group, and MCI and AD are marked by a loss in posterior connectivity (Damoiseaux et al., 2012; Hillary et al., 2015; Sheline and Raichle, 2013; Tijms et al., 2013). Given that a language deficit is an early sign of developing AD, future research should investigate whether these state-behavior relationships can be reliably observed in MCI as well as the implications that preservation of these states has for conversion to AD.

Acknowledgements

The manuscript does not represent the views of the Department of Veterans Affairs of the United States Government. This project was partially supported by VA Merit Review Award (IRX001534), SPiRE (IRX001381), and Career Development Award (B6366W) as well as the NIH/NIA funded Michigan Alzheimer's Disease Center (5P30AG053760) and the Alzheimer's Disease Research Center, Emory University (2P50AG025688).

Conflict of interest

Einat K. Brenner, Benjamin M. Hampstead, Emily C. Grossner, Rachel A. Bernier, Nicholas Gilbert, K. Sathian, and Frank G. Hillary declare that they have no conflicts of interest.

Informed consent

All procedures followed were in accordance with the ethical standards of the responsible committee on human experimentation (institutional and national) and with the Helsinki Declaration of 1975, and the applicable revisions at the time of the investigation. Informed consent was obtained from all patients for being included in the study.

Appendix C. Supplementary data

Supplementary data to this article can be found online at https://doi.org/10.1016/j.ijpsycho.2018.05.001.

References

Abou-Elseoud, A., Starck, T., Remes, J., Nikkinen, J., Tervonen, O., Kiviniemi, V., 2010. The effect of model order selection in group PICA. Hum. Brain Mapp. 31, 1207–1216.
Agosta, F., Pievani, M., Geroldi, C., Copetti, M., Frisoni, G.B., Filippi, M., 2012. Resting state fMRI in Alzheimer's disease: beyond the default mode network. Neurobiol. Aging 33, 1564–1578.
Albert, M.S., DeKosky, S.T., Dickson, D., Dubois, B., Feldman, H.H., Fox, N.C., et al., Snyder, P.J., 2011. The diagnosis of mild cognitive impairment due to Alzheimer's disease: recommendations from the National Institute on Aging-Alzheimer's Association workgroups on diagnostic guidelines for Alzheimer's disease. Alzheimers Dement. 7, 270–279.
Allen, E.A., Damaraju, E., Plis, S.M., Erhardt, E.B., Eichele, T., Calhoun, V.D., 2014. Tracking whole-brain connectivity dynamics in the resting state. Cereb. Cortex 24, 663–676.
Badhwar, A., Tam, A., Dansereau, C., Orban, P., Hoffstaedter, F., Bellec, P., 2017. Resting-state network dysfunction in Alzheimer's disease: a systematic review and meta-analysis. Alzheimers Dement. 8, 73–85.
Bai, F., Shi, Y., Yuan, Y., Wang, Y., Yue, C., Teng, Y., et al., Zhang, Z., 2012. Altered self-referential network in resting-state amnestic type mild cognitive impairment. Cortex 48, 604–613.
Bassett, D.S., Bullmore, E.D., 2006. Small-world brain networks. Neuroscientist 12, 512–523.
Beharelle, A.R., Kovačević, N., McIntosh, A.R., Levine, B., 2012. Brain signal variability relates to stability of behavior after recovery from diffuse brain injury. NeuroImage 60, 1528–1537.
Bernier, R.A., Roy, A., Venkatesan, U.M., Grossner, E.C., Brenner, E.K., Hillary, F.G., 2017. Dedifferentiation does not account for hyperconnectivity after traumatic brain injury. Front. Neurol. 8, 297.
Binnewijzend, M.A., Schoonheim, M.M., Sanz-Arigita, E., Wink, A.M., van der Flier, W.M., Tolboom, N., et al., Barkhof, F., 2012. Resting-state fMRI changes in Alzheimer's disease and mild cognitive impairment. Neurobiol. Aging 33, 2018–2028.
Biswal, B., Zerrin Yetkin, F., Haughton, V.M., Hyde, J.S., 1995. Functional connectivity in the motor cortex of resting human brain using echo-planar mri. Magn. Reson. Med. 34, 537–541.
Bondi, M.W., Monsch, A.U., Butters, N., Salmon, D.P., Paulsen, J.S., 1993. Utility of a modified version of the Wisconsin Card Sorting Test in the detection of dementia of the Alzheimer type. Clin. Neuropsychol. 7, 161–170.
Braun, U., Schäfer, A., Bassett, D.S., Rausch, F., Schweiger, J.I., Bilek, E., et al., Haddad, L., 2016. Dynamic brain network reconfiguration as a potential schizophrenia genetic risk mechanism modulated by NMDA receptor function. Proc. Natl. Acad. Sci. 113, 12568–12573.
Brier, M.R., Thomas, J.B., Snyder, A.Z., Benzinger, T.L., Zhang, D., Raichle, M.E., et al., Ances, B.M., 2012. Loss of intranetwork and internetwork resting state functional connections with Alzheimer's disease progression. J. Neurosci. 32, 8890–8899.
Cabeza, R., Dennis, N.A., 2012. Frontal lobes and aging. In: Principles of Frontal Lobe Function, 2nd ed. Oxford University Press, New York, pp. 628–652.
Caccappolo-Van Vliet, E., Manly, J., Tang, M.X., Marder, K., Bell, K., Stern, Y., 2003. The neuropsychological profiles of mild Alzheimer's disease and questionable dementia as compared to age-related cognitive decline. J. Int. Neuropsychol. Soc. 9, 720–732.
Calhoun, V.D., Liu, J., Adali, T., 2009. A review of group ICA for fMRI data and ICA for joint inference of imaging, genetic, and ERP data. NeuroImage 45, S163–S172.
Chang, C., Glover, G.H., 2010. Time–frequency dynamics of resting-state brain connectivity measured with fMRI. NeuroImage 50, 81–98.
Cole, M.W., Schneider, W., 2007. The cognitive control network: integrated cortical regions with dissociable functions. NeuroImage 37, 343–360.
Cordes, D., Haughton, V.M., Arfanakis, K., Wendt, G.J., Turski, P.A., Moritz, C.H., et al., Meyerand, M.E., 2000. Mapping functionally related regions of brain with functional

connectivity MR imaging. Am. J. Neuroradiol. 21, 1636–1644.
Damoiseaux, J.S., Prater, K.E., Miller, B.L., Greicius, M.D., 2012. Functional connectivity tracks clinical deterioration in Alzheimer's disease. Neurobiol. Aging 33 (828-e19).
de Haan, W., Pijnenburg, Y.A., Strijers, R.L., van der Made, Y., van der Flier, W.M., Scheltens, P., Stam, C.J., 2009. Functional neural network analysis in frontotemporal dementia and Alzheimer's disease using EEG and graph theory. BMC Neurosci. 10, 101.
Dennis, N.A., Cabeza, R., 2008. Neuroimaging of healthy cognitive aging. In: The Handbook of Aging and Cognition. 3. pp. 1–54.
Dennis, E.L., Thompson, P.M., 2014. Functional brain connectivity using fMRI in aging and Alzheimer's disease. Neuropsychol. Rev. 24, 49–62.
Desikan, R.S., Ségonne, F., Fischl, B., Quinn, B.T., Dickerson, B.C., Blacker, D., et al., Albert, M.S., 2006. An automated labeling system for subdividing the human cerebral cortex on MRI scans into gyral based regions of interest. NeuroImage 31, 968–980.
Dickerson, B.C., Sperling, R.A., 2008. Functional abnormalities of the medial temporal lobe memory system in mild cognitive impairment and Alzheimer's disease: insights from functional MRI studies. Neuropsychologia 46, 1624–1635.
Fischer, P., Jungwirth, S., Zehetmayer, S., Weissgram, S., Hoenigschnabl, S., Gelpi, E., et al., Tragl, K.H., 2007. Conversion from subtypes of mild cognitive impairment to Alzheimer dementia. Neurology 68, 288–291.
Gilbert, N., Bernier, R.A., Calhoun, V.D., Brenner, E.K., Grossner, E.C., Rajtmajer, S.M., Hillary, F.G., 2018. Diminished network dynamics after moderate and severe traumatic brain injury. PLOS ONE (in press).
Gusnard, D.A., Raichle, M.E., 2001. Searching for a baseline: functional imaging and the resting human brain. Nat. Rev. Neurosci. 2, 685–694.
Hillary, F.G., Grafman, J.H., 2017. Injured brains and adaptive networks: the benefits and costs of hyperconnectivity. Trends Cogn. Sci. 21, 385–401.
Hillary, F.G., Genova, H.M., Chiaravalloti, N.D., Rypma, B., DeLuca, J., 2006. Prefrontal modulation of working memory performance in brain injury and disease. Hum. Brain Mapp. 27, 837–847.
Hillary, F.G., Roman, C.A., Venkatesan, U., Rajtmajer, S.M., Bajo, R., Castellanos, N.D., 2015. Hyperconnectivity is a fundamental response to neurological disruption. Neuropsychology 29, 59.
Hutchison, R.M., Womelsdorf, T., Gati, J.S., Everling, S., Menon, R.S., 2013. Resting state networks show dynamic functional connectivity in awake humans and anesthetized macaques. Hum. Brain Mapp. 34, 2154–2177.
Jones, D.T., Knopman, D.S., Gunter, J.L., Graff-Radford, J., Vemuri, P., Boeve, B.F., et al., Jack, C.R., 2016. Cascading network failure across the Alzheimer's disease spectrum. Brain 139, 547–562.
Kiviniemi, V., Starck, T., Remes, J., Long, X., Nikkinen, J., Haapea, M., et al., Tervonen, O., 2009. Functional segmentation of the brain cortex using high model order group PICA. Hum. Brain Mapp. 30, 3865–3886.
Li, R., Wu, X., Chen, K., Fleisher, A.S., Reiman, E.M., Yao, L., 2013. Alterations of directional connectivity among resting-state networks in Alzheimer disease. Am. J. Neuroradiol. 34, 340–345.
Liang, X., Zou, Q., He, Y., Yang, Y., 2013. Coupling of functional connectivity and regional cerebral blood flow reveals a physiological basis for network hubs of the human brain. Proc. Natl. Acad. Sci. 110, 1929–1934.
Liegeois, R., Laumann, T.O., Snyder, A.Z., Zhou, J., Yeo, B.T., 2017. Interpreting temporal fluctuations in resting-state functional connectivity MRI. NeuroImage 163, 437–455.
Lindquist, M.A., 2008. The statistical analysis of fMRI data. Stat. Sci. 439–464.
Lloyd, S., 1982. Least squares quantization in PCM. IEEE Trans. Inf. Theory 28, 129–137.
Lukatela, K., Malloy, P., Jenkins, M., Cohen, R., 1998. The naming deficit in early Alzheimer's and vascular dementia. Neuropsychology 12, 565.
Martin, A., Fedio, P., 1983. Word production and comprehension in Alzheimer's disease: the breakdown of semantic knowledge. Brain Lang. 19, 124–141.
Mayer, A.R., Ling, J.M., Allen, E.A., Klimaj, S.D., Yeo, R.A., Hanlon, F.M., 2015. Static and dynamic intrinsic connectivity following mild traumatic brain injury. J. Neurotrauma 32, 1046–1055.
Medaglia, J.D., 2017. Functional neuroimaging in traumatic brain injury: from nodes to networks. Front. Neurol. 8, 407.
Nagahama, Y., Okina, T., Suzuki, N., Matsuzaki, S., Yamauchi, H., Nabatame, H., Matsuda, M., 2003. Factor structure of a modified version of the Wisconsin card sorting test: an analysis of executive deficit in Alzheimer's disease and mild cognitive impairment. Dement. Geriatr. Cogn. Disord. 16, 103–112.
Nenadovic, V., Hutchison, J.S., Dominguez, L.G., Otsubo, H., Gray, M.P., Sharma, R., et al., Velazquez, J.L.P., 2008. Fluctuations in cortical synchronization in pediatric traumatic brain injury. J. Neurotrauma 25, 615–627.
Park, D.C., Reuter-Lorenz, P., 2009. The adaptive brain: aging and neurocognitive scaffolding. Annu. Rev. Psychol. 60, 173–196.
Petersen, R.C., 2004. Mild cognitive impairment as a diagnostic entity. J. Intern. Med. 256, 183–194.
Raichle, M.E., 2015. The brain's default mode network. Annu. Rev. Neurosci. 38, 433–447.
Raichle, M.E., MacLeod, A.M., Snyder, A.Z., Powers, W.J., Gusnard, D.A., Shulman, G.L., 2001. A default mode of brain function. Proc. Natl. Acad. Sci. 98, 676–682.
Rashid, B., Damaraju, E., Pearlson, G.D., Calhoun, V.D., 2014. Dynamic connectivity states estimated from resting fMRI identify differences among schizophrenia, bipolar disorder, and healthy control subjects. Front. Hum. Neurosci. 8, 897.
Rombouts, S.A., Barkhof, F., Goekoop, R., Stam, C.J., Scheltens, P., 2005. Altered resting state networks in mild cognitive impairment and mild Alzheimer's disease: an fMRI study. Hum. Brain Mapp. 26, 231–239.
Roy, A., Bernier, R.A., Wang, J., Benson, M., French Jr., J.J., Good, D.C., Hillary, F.G., 2017. The evolution of cost-efficiency in neural networks during recovery from traumatic brain injury. PLoS One 12, e0170541.
Sheline, Y.I., Raichle, M.E., 2013. Resting state functional connectivity in preclinical Alzheimer's disease. Biol. Psychiatry 74, 340–347.
Smith, S.M., Jenkinson, M., Woolrich, M.W., Beckmann, C.F., Behrens, T.E., Johansen-Berg, H., et al., Niazy, R.K., 2004. Advances in functional and structural MR image analysis and implementation as FSL. NeuroImage 23, S208–S219.
Smith, S.M., Fox, P.T., Miller, K.L., Glahn, D.C., Fox, P.M., Mackay, C.E., et al., Beckmann, C.F., 2009. Correspondence of the brain's functional architecture during activation and rest. Proc. Natl. Acad. Sci. 106, 13040–13045.
Sorg, C., Riedl, V., Mühlau, M., Calhoun, V.D., Eichele, T., Läer, L., et al., Wohlschläger, A.M., 2007. Selective changes of resting-state networks in individuals at risk for Alzheimer's disease. Proc. Natl. Acad. Sci. 104, 18760–18765.
Tijms, B.M., Wink, A.M., de Haan, W., van der Flier, W.M., Stam, C.J., Scheltens, P., Barkhof, F., 2013. Alzheimer's disease: connecting findings from graph theoretical studies of brain networks. Neurobiol. Aging 34, 2023–2036.
van den Heuvel, M.P., Sporns, O., 2013. Network hubs in the human brain. Trends Cogn. Sci. 17, 683–696.
Wang, J., Zuo, X., Dai, Z., Xia, M., Zhao, Z., Zhao, X., et al., He, Y., 2013. Disrupted functional brain connectome in individuals at risk for Alzheimer's disease. Biol. Psychiatry 73, 472–481.
Williams, B.W., Mack, W., Henderson, V.W., 1989. Boston naming test in Alzheimer's disease. Neuropsychologia 27, 1073–1079.